Spectroscopic measurements of hydrogen dissociation degree and H^- production in resonant antenna-generated helicon plasmas

C. Marini[1], B. P. Duval[1], I. Furno[1], A. A. Howling[1], R. Jacquier[1], A. N. Karpushov[1], Ph. Guittienne[2], U. Fantz[3], D. Wünderlich[3], S. Béchu[4], and A. Simonin[5]

[1]EPFL, Swiss Plasma Center (SPC), CH-1015 Lausanne, Switzerland.

[2]Helyssen, Route de la Louche 31, CH-1092 Belmont-sur-Lausanne, Switzerland.

[3]Max-Planck-Institut fuer Plasmaphysik, Boltzmannstr. 2, 85748 Garching, Germany.

[4]LPSC, Université Grenoble-Alpes, CNRS/IN2P3, F-38026 Grenoble, France.

[5]CEA, IRFM, F-13108 St Paul lez Durance, France.

Introduction

A new generation of neutral beam (NB) systems will be required in fusion reactors, such as DEMO, able to deliver up to 50 MW of high neutral particle energy (0.8-1 MeV) with high wall-plug efficiency (≃60%). Negative ion beams can access this performance, resulting in a strong research focus on negative ion production from surface or volumetric plasma sources. A novel helicon plasma source, based on a resonant birdcage network antenna [1], is currently under study at the Swiss Plasma Center (SPC), before installation on the Cybele negative ion source [2] at CEA-IRFM. This paper reports on passive spectroscopic measurements of the absolute intensity of the Balmer H_α, H_β and H_γ and the diagonal Fulcher-α lines. These are analysed using the collisional radiative code YACORA [4] to estimate the hydrogen dissociation degree and the H^- density.

Experimental setup

Figure 1 shows a CAD drawing of the Resonant Antenna Ion Device (RAID) together with the input optics for the reported spectroscopic measurements. RAID is a 1.8 m long linear device, with a 40 cm diameter circular cross section and equipped with 6 magnetic field coils. The helicon antenna, able to deliver up to 10 kW at 13.56 MHz, is installed at one end outside the main coil region. The coil current is $I_{coil} = 150$ A , for a nominal field on axis of 150 G, while the current on the first coil

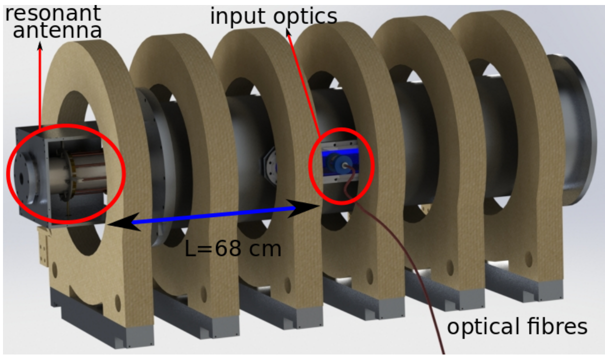

Figure 1: *3D CAD drawing of RAID, with the input optics for spectroscopic measurements.*

is reversed, $I_{coil1} = -30$ A, to increase the B gradient. These experimental conditions $B = 150$ G and neutral gas pressure $p \leq 0.3$ Pa meet the specifications of the Cybele source [2]. The spectroscopic setup consists of a field lens, an optical fibre bundle, a high throughput spectrometer and a detector. The input optics is a Navitar f/1.4 35mm lens with an image focal plane at 25 cm from the lens, i.e. the RAID axis. There are 19 fibres of numerical aperture 0.22 and with a fused silica core of diameter 365 μm. The diameter of their image on the focal plane is 2.9 mm, resulting in a sampling region $\simeq$ 55 mm wide. To perform measurements at a relevant impact parameter, up to 8 cm, two set of measurements with different viewing angle were required. The viewline geometry was verified by back illuminating each fibre with a He/Ne laser and measuring the spot position on a reference anti-reflection graphite ring installed inside the vacuum vessel.

Collected light is analysed by a spectrometer, composed of two Nikon f/2 200 mm lenses and a holographic grating blazed at 400 nm of size 120x140 mm^2. The spectrometer input slit width is set to 80 μm for a spectral bandpass of 0.9 Å at 615 nm sufficient to resolve most of the Fulcher-α molecular lines. The detector is an Andor camera iXon Ultra 897, with a back-illuminated 512x512 pixels frame transfer sensor and an optional electron multiplying EM readout register. The camera integration time and EM gain are adjusted at each scanning angle to maximise the counts and S/N ratio whilst avoiding saturation.

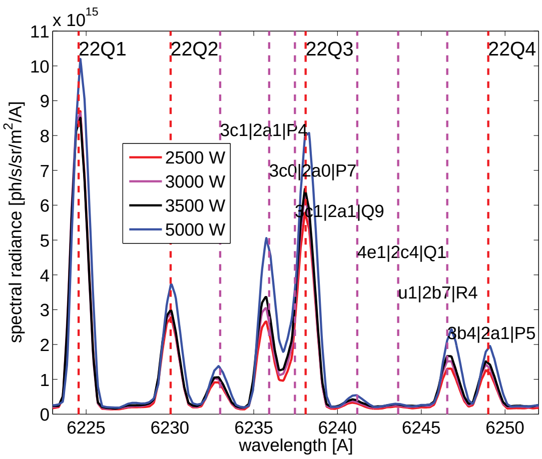

Figure 2: *H_2 spectrum of Fulcher-α 22QN lines for different RF powers.*

Radiance and emissivity profiles

Measurements in both H_2 and D_2 were performed but in this paper, only H_2 data is presented. The light of each optical fibre is imaged to a region of interest (ROI) on the CCD, the photon rate R_{exp} [ph/s] of each emitted line for each ROI is evaluated using a multi-gaussian fitting, that accounts for the experimental instrumental function. The absolute radiance is then deduced by comparing the experimental rate R_{exp} with the photon rate R_{cal} measured with an absolutely calibrated source at the same wavelength, using the same setup. This ensures correct compensation for the system transmission and etendue. The radiance [ph/s/sr/m^2] of a line is then $L_{exp} = \frac{R_{exp}}{R_{cal}} L_{cal}$, where L_{cal} is the known radiance of the calibration source. An example of a molecular spectrum in the range of the 22QN (N from 1 to 4) lines is shown in Fig. 2,

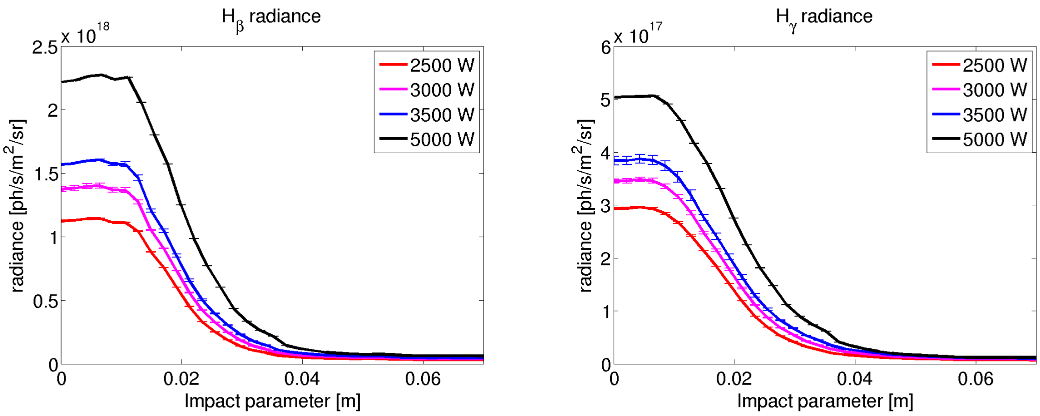

Figure 3: *H_β and H_γ radiance profile for different RF powers.*

where the molecular lines are identified comparing their wavelength with Ref. [3]. Figure 3 shows the resulting radiance profiles for the Balmer H_β and H_γ lines respectively. The radiance of each line increases almost linearly with the input power, with constant profile shape. A minimum Fisher regularisation algorithm is then applied to calculate the absolute emissivity profile for each emission line, in cylindrical symmetry as experimentally observed. The correct convergence of the algorithm is verified by reconstructing the input radiance profiles from the output emissivities. An error estimate of the Abel-inverted profiles is performed using a Monte Carlo approach. Figure 4 shows the case of H_γ line, similar features are observed for the other lines as well, in particular emissivity profiles are generally hollow and their shape is similar at different input powers.

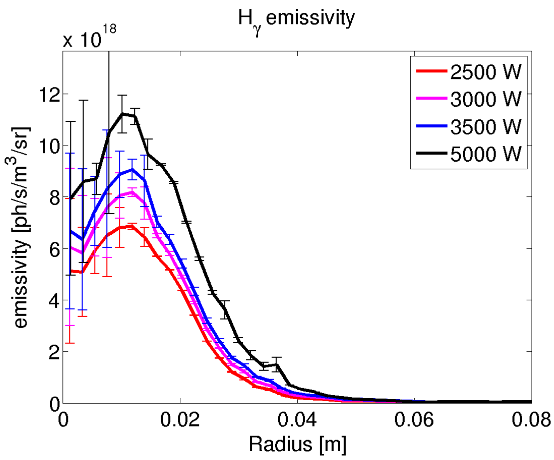

Figure 4: *H_γ emissivity profile for different RF powers.*

Analysis and results

The first 3 Balmer lines and the sum of the diagonal Fulcher-α lines profiles are interpreted here using the collisional-radiative code YACORA [4]. As an example, the output n_e and T_e profiles are compared in Fig. 5 with experimental profiles, measured with an RF-compensated Langmuir probe (LP), at 3kW input power. The T_e profile is in agreement while there is a discrepancy of about a factor 1.7 in the n_e profile that is still under investigation. The gas translational and vibrational temperatures can be estimated from the Fulcher lines and are respectively $T_{tran} = 900 \pm 200$ K and $T_{vib} \geq 6000$ K. Figure 6 show the dissociation fraction $f_d = n_H/n_{H_2}$

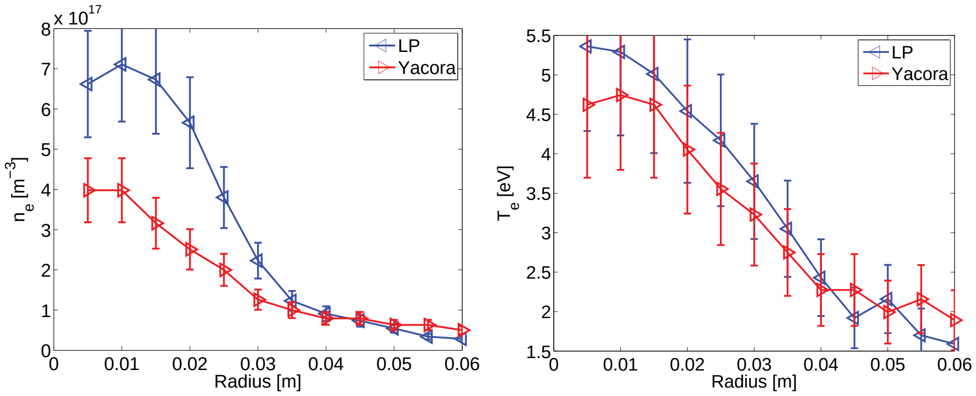

Figure 5: *Comparison of experimental n_e and T_e profiles (LP) with YACORA convergence values for input power 3 kW.*

profile in blue and the ratio $f_{neg} = n_{H^-}/n_e$ in red, for the 3kW case.

The f_d profile reaches interestingly high values for use as a negative ion surface source, with a dissociation degree $\alpha = \frac{f_d}{f_d+2}$ up to 33%. The ratio f_{neg} is lower than 0.05 inside the plasma column (radius < 2 cm), where the relatively high T_e prevents a stable formation of H^-. Interestingly, f_{neg} increases at the edge of the plasma column $3 \leq r \leq 4$ cm, resulting in the high value of $n_{H^-} \simeq 4 \cdot 10^{16}$ m^{-3}. In conclusion, the dissociation degree is fairly constant in the range 25%-33% at a relatively low power of 3 kW. This performances are promising for application of the helicon antenna as a high efficiency plasma source for the Cybele NIB.

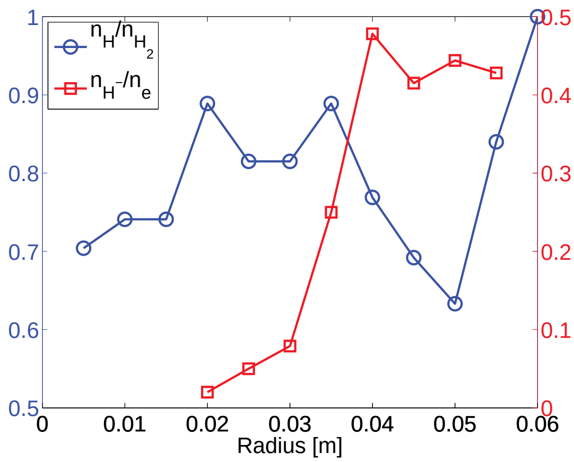

Figure 6: *Profiles of the ratios $f_d = n_H/n_{H_2}$ and $f_{neg} = n_{H^-}/n_e$ from YACORA.*

This work has been carried out within the framework of the EUROfusion Consortium and has received funding from the Euratom research and training programme 2014-2018 under grant agreement No 633053. The views and opinions expressed herein do not necessarily reflect those of the European Commission.

References

[1] Ph. Guittienne and E. Chevalier, *J. Appl. Phys.*, **98**, 083304 (2005)

[2] A. Simonin et al., *Nucl. Fusion* **55**, 123020 (2015)

[3] G.H. Dieke, The hydrogen molecule wavelength tables of G. H. Dieke, Crosswhite (1972)

[4] D. Wunderlich, S. Dietrich, U. Fantz, *J. Quant. Spectros. Radia. Transfer* **110**, 62-71 (2009)